

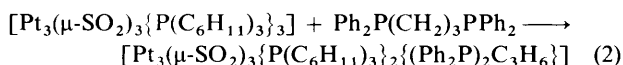
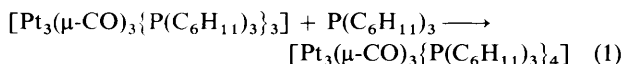
Facilitation of the Substitution Reactions of Triangular Platinum Cluster Compounds and the Structural Characterisations of $[\text{Pt}_3(\mu\text{-SO}_2)_3\{\text{P}(\text{C}_6\text{H}_{11})_3\}_3]$ and $[\text{NEt}_4][\text{Pt}_3(\mu\text{-Br})(\mu\text{-SO}_2)_2\{\text{P}(\text{C}_6\text{H}_{11})_3\}_3]$ by Single-crystal X-Ray Techniques†

Simon G. Bott, Malcolm F. Hallam, Osayi J. Ezomo, D. Michael P. Mingos,* and Ian D. Williams
Inorganic Chemistry Laboratory, University of Oxford, South Parks Road, Oxford OX1 3QR

Trimethylamine *N*-oxide has been used to facilitate the substitution reactions of the *triangulo*-triplatinum clusters $[\text{Pt}_3(\mu\text{-SO}_2)_3(\text{PR}_3)_3]$ ($\text{R} = \text{cyclo-C}_6\text{H}_{11}$ or Ph) with CO, halide, and azide anions. In the absence of Me_3NO a benzene solution of $[\text{Pt}_3(\mu\text{-SO}_2)_3\{\text{P}(\text{C}_6\text{H}_{11})_3\}_3]$ gives only partially substituted products with CO, but the addition of Me_3NO leads to a high-yield conversion to $[\text{Pt}_3(\text{CO})_3\{\text{P}(\text{C}_6\text{H}_{11})_3\}_3]$. Me_3NO has also been used to synthesise some unusual 44-electron anionic clusters of the general type $[\text{Pt}_3(\mu\text{-X})(\mu\text{-SO}_2)_2(\text{PR}_3)_3]^-$ [$\text{X} = \text{Cl}, \text{Br}$, or N_3 ; $\text{PR}_3 = \text{P}(\text{C}_6\text{H}_{11})_3$, PPh_3 , or PMe_2Ph]. The compounds have been characterised by i.r. spectroscopy and $^{31}\text{P}\{-^1\text{H}\}$ and $^{195}\text{Pt}\{-^1\text{H}\}$ n.m.r. studies. Single-crystal X-ray crystallographic investigations of the related 42- and 44-valence electron clusters $[\text{Pt}_3(\mu\text{-SO}_2)_3\{\text{P}(\text{C}_6\text{H}_{11})_3\}_3]$ and $[\text{NEt}_4][\text{Pt}_3(\mu\text{-Br})(\mu\text{-SO}_2)_2\{\text{P}(\text{C}_6\text{H}_{11})_3\}_3]$ have demonstrated that the additional electron pair causes an expansion of the Pt_3 triangle, with the average Pt–Pt distance increasing from 2.814(1) to 2.885 4(15) Å.

The facilitation of substitution reactions of metal carbonyl complexes by trimethylamine *N*-oxide (Me_3NO) is well documented and has proved to be particularly efficient for compounds where the CO stretching frequency exceeds 2000 cm^{-1} .^{1,2} Since Me_3NO is known to react with SO_2 to form the adduct Me_3NSO_2 ³ we have investigated the effect of Me_3NO on the substitution reactions of triangular platinum clusters of the type $[\text{Pt}_3(\mu\text{-SO}_2)_3(\text{PR}_3)_3]$; a preliminary account is given in ref. 4.

The cluster chemistry of platinum has been the subject of considerable recent interest (see ref. 5 for a review) and yielded examples of compounds with 3–38 metal atoms. The majority of low-nuclearity platinum clusters contain a combination of phosphine and either CO ,⁶ SO_2 ,⁷ or $\text{CNC}_6\text{H}_4\text{Me}_2$ -2,6⁸ ligands and many examples have been structurally characterised.⁵ A common structural feature of these platinum clusters is the Pt_3 triangular unit, which is found either in isolation in 42- and 44-electron clusters or fused to other polyhedral fragments. Theoretical calculations on triangular platinum clusters^{9,10} have indicated that their ability to support the alternative electron counts of 42 and 44 resides in the presence of low-lying orbitals of a_2' and a_2'' symmetry. The latter is stabilised by cylindrical π -acceptor ligands such as CO, leading for example to $[\text{Pt}_3(\mu\text{-CO})_3(\text{CO})_3]^{2-}$ which is the 44-electron precursor to the stacked platinum clusters of Chini and co-workers,¹¹ and the former by both π -donors and π -acceptors, e.g. SO_2 and PPh_2 . Although the 42- to 44-electron transformation has been observed for monodentate and bidentate phosphines, equations (1)¹² and (2)¹³ ($\text{C}_6\text{H}_{11} = \text{cyclohexyl}$), it involves



† 1,2,1,3;2,3-Tri- μ -(sulphur dioxide-*S*)-1,2,3-tris(tricyclohexylphosphine)-*triangulo*-triplatinum and tetraethylammonium 1,2- μ -bromo-1,3;2,3-di- μ -(sulphur dioxide-*S*)-1,2,3-tris(tricyclohexylphosphine)-*triangulo*-triplatinate(1-) respectively.

Supplementary data available: see Instructions for Authors, *J. Chem. Soc., Dalton Trans.*, 1988, Issue 1, pp. xvii–xx.

Non-S.I. unit employed: atm = 101 325 Pa.

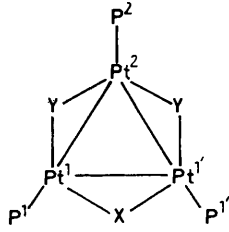
only a change in the number of terminal ligands. In this paper we describe how such transformations can be achieved by substitution reactions involving the bridging ligands.

Results and Discussion

The reaction of $[\text{Pt}_3(\mu\text{-CO})_3\{\text{P}(\text{C}_6\text{H}_{11})_3\}_3]$ (**1**)¹⁴ with SO_2 at 1 atm pressure and 60 °C in benzene results in the complete replacement of the CO ligands and the cluster $[\text{Pt}_3(\mu\text{-SO}_2)_3\{\text{P}(\text{C}_6\text{H}_{11})_3\}_3]$ (**2**) is obtained in 65% yield.⁷ When (**2**) is treated with CO the reaction is not reversed and the major product is $[\text{Pt}_3(\mu\text{-SO}_2)(\mu\text{-CO})_2\{\text{P}(\text{C}_6\text{H}_{11})_3\}_3]$ (**3**). Small quantities of $[\text{Pt}_2(\mu\text{-SO}_2)(\text{CO})_2\{\text{P}(\text{C}_6\text{H}_{11})_3\}_2]$ also resulted from the reaction. Even when the temperature was raised to 60 °C and the reaction left for extended periods of time, conversion to the fully substituted derivative was not observed. Addition of Me_3NO to a solution of (**2**) in benzene under CO at 1 atm pressure led to the isolation of the fully substituted clusters $[\text{Pt}_3(\mu\text{-CO})_3\{\text{P}(\text{C}_6\text{H}_{11})_3\}_3]$ in high yield (>90%) even at room temperature. The extent of acceleration of the rate of the reaction by Me_3NO depended on the mole ratio: 3 mol equiv. Me_3NO required a reaction time of 6–8 h, and 20 mol equiv., 2–3 h for complete conversion.

The accelerating effect of Me_3NO has also been utilised in the synthesis of a new class of anionic 44-electron triangular cluster compounds of platinum with bridging halide and bridging azido-ligands. The addition of quaternary ammonium halide salts $[\text{NEt}_3(\text{CH}_2\text{Ph})]\text{Cl}$ or $[\text{NEt}_4]\text{Br}$ in ethanol to benzene solutions of $[\text{Pt}_3(\mu\text{-SO}_2)_3(\text{PPh}_3)_3]$ gives high yields (>80%) of the salts $[\text{NEt}_3(\text{CH}_2\text{Ph})][\text{Pt}_3(\mu\text{-Cl})(\mu\text{-SO}_2)_2(\text{PPh}_3)_3]$ (**4a**) and $[\text{NEt}_4][\text{Pt}_3(\mu\text{-Br})(\mu\text{-SO}_2)_2(\text{PPh}_3)_3]$ (**4b**) respectively. The corresponding reactions of $[\text{Pt}_3(\mu\text{-SO}_2)_3\{\text{P}(\text{C}_6\text{H}_{11})_3\}_3]$ with $[\text{NEt}_4]\text{Cl}$ and $[\text{NEt}_4]\text{Br}$ are very slow and are incomplete even after 2 d. The addition of Me_3NO (3 mol equiv.) leads to complete conversion to $[\text{NEt}_4][\text{Pt}_3(\mu\text{-X})(\mu\text{-SO}_2)_2\{\text{P}(\text{C}_6\text{H}_{11})_3\}_3]$ (**4c**, $\text{X} = \text{Cl}$; **4d**, $\text{X} = \text{Br}$) after 15 min at room temperature. $[\text{Pt}_3(\mu\text{-SO}_2)_3\{\text{P}(\text{C}_6\text{H}_{11})_3\}_3]$ also reacts slowly with $[\text{N}(\text{PPh}_3)_2]\text{N}_3$ to give $[\text{N}(\text{PPh}_3)_2][\text{Pt}_3(\mu\text{-N}_3)(\mu\text{-SO}_2)_2\{\text{P}(\text{C}_6\text{H}_{11})_3\}_3]$ (**4e**) in 75% yield after 18 h at room temperature. Addition of Me_3NO to this reaction led to an acceleration of the rate but resulted in additional side reactions and a mixture of products which could not be characterised using $^{31}\text{P}\{-^1\text{H}\}$ n.m.r.

The complex $[\text{Pt}_3(\mu\text{-SO}_2)_3(\text{PMe}_2\text{Ph})_3]$ ⁷ reacts rapidly with

Table 1. Chemical shifts and coupling constants for $[\text{Pt}_3(\mu\text{-X})(\mu\text{-Y})_2(\text{PR}_3)_3]$ clusters


Compound anion	$\delta/\text{p.p.m.}$				J/Hz							
	^{31}P		^{195}Pt		$^1J_{\text{Pt-P}}$		$^1J_{\text{Pt-Pt}}$		$^2J_{\text{Pt-P}}$		$^3J_{\text{P-P}}$	
	P ¹	P ²	Pt ¹	Pt ²	1-1	2-2	1-2	1-1'	1-2	2-1	1-1'	1-2
(3) $[\text{Pt}_3(\mu\text{-SO}_2)(\mu\text{-CO})_2\{\text{P}(\text{C}_6\text{H}_{11})_3\}_3]$	61.9	82.2	-4 515	-4 011	4 055	5 134	1 830	301	449	372	51	62
(4a) $[\text{Pt}_3(\mu\text{-Cl})(\mu\text{-SO}_2)_2(\text{PPh}_3)_3]^-$	17.3	4.0			5 469	4 599		300	431	345	46	62
(4b) $[\text{Pt}_3(\mu\text{-Br})(\mu\text{-SO}_2)_2(\text{PPh}_3)_3]^-$	19.3	7.6			5 482	4 620		303	440	350	47	62
(4c) $[\text{Pt}_3(\mu\text{-Cl})(\mu\text{-SO}_2)_2\{\text{P}(\text{C}_6\text{H}_{11})_3\}_3]^-$	28.9	12.9	-4 653	-5 997	4 963	4 341	968	245	352	314	45	59
(4d) $[\text{Pt}_3(\mu\text{-Br})(\mu\text{-SO}_2)_2\{\text{P}(\text{C}_6\text{H}_{11})_3\}_3]^-$	31.7	15.9	-4 650	-5 990	4 972	4 345	970	240	353	307	48	59
(4e) $[\text{Pt}_3(\mu\text{-N}_3)(\mu\text{-SO}_2)_2\{\text{P}(\text{C}_6\text{H}_{11})_3\}_3]^-$	28.3	13.6			4 973	4 325		237	345	300	47	59
(4f) $[\text{Pt}_3(\mu\text{-Cl})(\mu\text{-SO}_2)_2(\text{PMe}_2\text{Ph})_3]^-$	-10.8	-25.8			5 325	4 455		285	399	320	46	60

$[\text{N}(\text{PPh}_3)_2]\text{Cl}$ to give $[\text{N}(\text{PPh}_3)_2][\text{Pt}_3(\mu\text{-Cl})(\mu\text{-SO}_2)_2(\text{PMe}_2\text{-Ph})_3]$ (**4f**) in 80% yield after 10 min. Therefore, it was not necessary to add Me_3NO to accelerate the reaction. The observation that the relative rates of substitution for the $[\text{Pt}_3(\mu\text{-SO}_2)_3(\text{PR}_3)_3]$ clusters is $\text{PMe}_2\text{Ph} > \text{PPh}_3 > \text{P}(\text{C}_6\text{H}_{11})_3$ suggests that steric factors are important and that the reactions proceed through a 44-electron intermediate, $[\text{Pt}_3\text{X}(\mu\text{-SO}_2)_3(\text{PR}_3)_3]^-$.

The $^{31}\text{P}\{-^1\text{H}\}$ and $^{195}\text{Pt}\{-^1\text{H}\}$ n.m.r. data for compounds (**3**) and (**4a**)—(**4f**) are summarised in Table 1. These compounds which have C_{2v} symmetries show two resonances in the ratio of 2:1 in their $^{31}\text{P}\{-^1\text{H}\}$ and $^{195}\text{Pt}\{-^1\text{H}\}$ n.m.r. spectra. The observed spectra were satisfactorily simulated using the following spin systems which take into account the platinum isotopomer distribution: A_2B (29.1%, no ^{195}Pt nuclei); A_2BX (14.8%, one ^{195}Pt nucleus in the unique symmetry position); $AA'BY$ (29.6%, one ^{195}Pt nucleus in one of the symmetry related positions); $AA'BXY$ (15.1%, two ^{195}Pt nuclei in symmetry inequivalent positions); $AA'BXX'$ (7.5%, two ^{195}Pt nuclei in symmetry equivalent positions); $AA'BXX'Y$ (3.8%, three ^{195}Pt nuclei). The compounds consistently show a smaller $^1J_{\text{Pt-Pt}}$ coupling constant for the bond bridged by the unique ligand, i.e. for the bond bridged by either halide or SO_2 .

The anions $[\text{Pt}_3(\mu\text{-X})(\mu\text{-SO}_2)_2(\text{PR}_3)_3]^-$ (**4a**)—(**4f**) crystallise as pale yellow solids and have $\nu(\text{SO}_2)$ stretching modes in the ranges 1 149—1 226 $[\nu(\text{SO}_2)_{\text{asym}}]$ and 1 007—1 027 cm^{-1} $[\nu(\text{SO}_2)_{\text{sym}}]$ characteristic of bridging SO_2 ligands. In the parent compounds $[\text{Pt}_3(\mu\text{-SO}_2)_3(\text{PR}_3)_3]$ the corresponding frequencies are higher, suggesting more back donation to the bridging SO_2 ligands in the anionic compounds. The compound $[\text{Pt}_3(\mu\text{-N}_3)(\mu\text{-SO}_2)_2\{\text{P}(\text{C}_6\text{H}_{11})_3\}_3]^-$ (**4e**) shows an additional band at 2 051 cm^{-1} which is attributed to a bridging azido-ligand.¹⁵

In order to confirm the formulation of the anionic triangular clusters and to evaluate the structural changes which result from the substitution of SO_2 by halide in $[\text{Pt}_3(\mu\text{-SO}_2)\{\text{P}(\text{C}_6\text{H}_{11})_3\}_3]$ single-crystal X -ray crystallographic studies on $[\text{Pt}_3(\mu\text{-SO}_2)_3\{\text{P}(\text{C}_6\text{H}_{11})_3\}_3]$ and $[\text{NEt}_4][\text{Pt}_3(\mu\text{-Br})(\mu\text{-SO}_2)_2\{\text{P}(\text{C}_6\text{H}_{11})_3\}_3]$ were completed; the data are summarised in Table 2.

The molecular structure of $[\text{Pt}_3(\mu\text{-SO}_2)_3\{\text{P}(\text{C}_6\text{H}_{11})_3\}_3]$ is illustrated in Figure 1. The three platinum atoms approximate

Table 2. Data collection and structure solution parameters for the crystal structure determinations of (**2**) and (**4d**)

	(2)	(4d)
Compound	$\text{C}_{54}\text{H}_{99}\text{O}_6\text{P}_3\text{Pt}_3\text{S}_3 \cdot 2\text{C}_6\text{H}_6 \cdot \text{CH}_2\text{Cl}_2$	$\text{C}_{54}\text{H}_{99}\text{BrO}_4\text{P}_3\text{Pt}_3\text{S}_2 \cdot \text{C}_8\text{H}_{20}\text{N} \cdot 2\text{C}_6\text{H}_6$
M	1 853.7	1 921.1
Space group	$P2_1/n$	$Pnma$
Cell constants		
$a/\text{\AA}$	15.388(3)	27.982(5)
$b/\text{\AA}$	21.583(4)	27.310(4)
$c/\text{\AA}$	20.945(4)	10.235(2)
$\beta/^\circ$	93.30(1)	
$U/\text{\AA}^3$	6 944	7 822
Z	4	4
$D_c/\text{g cm}^{-3}$	1.78	1.63
Dimensions (mm)	0.35 \times 0.24 \times 0.26	0.40 \times 0.10 \times 0.07
$\mu(\text{Mo-K}\alpha)/\text{cm}^{-1}$	63.7	60.7
Scan technique	ω	ω
Scan width	0.8 + 0.35tan θ	0.7 + 0.35tan θ
Crystal decay	12%	3%
Total reflections	10 117	8 895
2θ Range ($^\circ$)	3—45	3—52
Observed reflections		
$I > 3\sigma(I)$	5 054	4 291
Max./min. absorption corrections	1.72/1.00	1.65/1.00
Number of parameters	381	388
Weighting scheme coefficients	99.25, 125.54, 43.05	5.77, -3.44, 4.24
R	0.058	0.044
R'	0.072	0.050

to an equilateral triangle and the Pt-Pt bond lengths (see Table 3) range from 2.813(1) to 2.815(1) \AA . These bond lengths are longer than those previously observed for the related Pt_3 cluster $[\text{Pt}_3(\mu\text{-SO}_2)_3(\text{PPh}_3)_3]$ [2.701(6) \AA]¹⁶ and the carbonyl-bridged cluster $[\text{Pt}_3(\mu\text{-CO})_3\{\text{P}(\text{C}_6\text{H}_{11})_3\}_3]$ [2.655(2) \AA].¹⁷ Steric repulsions between the SO_2 bridging ligands and the cyclohexyl rings which are arranged in an eclipsed fashion could make a substantial contribution to this observation. The short contacts between the SO_2 oxygen atoms and the β -carbons [av. 2.91(5) \AA] support this suggestion.

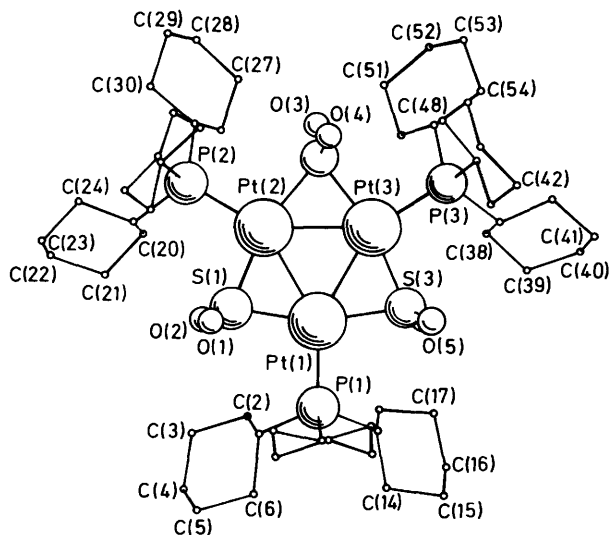


Figure 1. Structure and numbering scheme of $[\text{Pt}_3(\mu\text{-SO}_2)_3\{\text{P}(\text{C}_6\text{H}_{11})_3\}_3]$

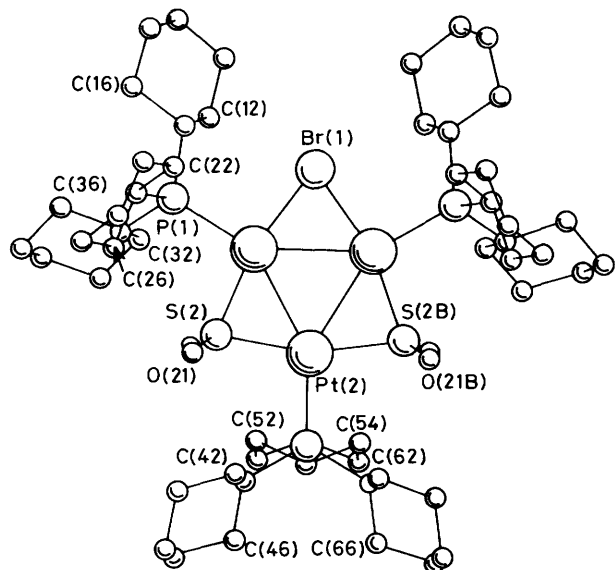


Figure 2. Structure and numbering scheme of $[\text{Pt}_3(\mu\text{-Br})(\mu\text{-SO}_2)_2\{\text{P}(\text{C}_6\text{H}_{11})_3\}_3]^-$ anion

The molecular structure of $[\text{NEt}_4][\text{Pt}_3(\mu\text{-Br})(\mu\text{-SO}_2)_2\{\text{P}(\text{C}_6\text{H}_{11})_3\}_3]$ (**4d**) is illustrated in Figure 2. The three platinum atoms also define a triangle, but the accuracy of the determination has been limited by crystallographic disorder involving the bridging SO_2 and Br ligands. This disorder means that it is impossible to comment specifically on the effect of bromide substitution on a Pt–Pt bond. Nevertheless, a general expansion of the triangle is observed. In $[\text{Pt}_3(\mu\text{-Br})(\mu\text{-SO}_2)_2\{\text{P}(\text{C}_6\text{H}_{11})_3\}_3]^-$ the triangle lies on a mirror plane and the two independent Pt–Pt distances are 2.882 6(8) and 2.886 8(8) Å (see Table 4 for a summary of important bond lengths). These bond lengths are significantly longer than those for the parent triangular cluster. In the related cluster compounds $[\text{Pt}_3\text{Au}(\mu\text{-Cl})(\mu\text{-SO}_2)_2\{\text{P}(\text{C}_6\text{H}_{11})_3\}_3(\text{PR}'_3)]$ and $[\text{Pt}_3\text{Au}_2(\mu\text{-Cl})(\mu\text{-SO}_2)_2\{\text{P}(\text{C}_6\text{H}_{11})_3\}_3(\text{PR}'_3)_2]^+$ ($\text{R}' = \text{C}_6\text{H}_4\text{F-p}$) where either one or

Table 3. Bond distances (Å) and angles (°) for compound (**2**)

Pt(1)–Pt(2)	2.814(1)	Pt(1)–Pt(3)	2.813(1)
Pt(2)–Pt(2)	2.815(1)	Pt(1)–P(1)	2.275(5)
Pt(2)–P(2)	2.298(6)	Pt(3)–P(3)	2.288(6)
Pt(1)–S(1)	2.268(7)	Pt(1)–S(3)	2.316(7)
Pt(2)–S(1)	2.255(7)	Pt(2)–S(2)	2.30(1)
Pt(3)–S(2)	2.291(9)	Pt(3)–S(3)	2.270(8)
S(1)–O(1)	1.44(3)	S(1)–O(2)	1.33(4)
S(2)–O(3)	1.2(1)	S(2)–O(4)	1.6(1)
S(3)–O(5)	1.38(4)	S(3)–O(6)	1.31(6)
Pt(2)–Pt(1)–Pt(3)	60.04(3)	Pt(1)–Pt(2)–Pt(3)	59.96(3)
Pt(1)–Pt(3)–Pt(2)	60.00(3)	Pt(2)–Pt(1)–P(1)	150.4(2)
Pt(3)–Pt(1)–P(1)	148.9(2)	Pt(1)–Pt(2)–P(2)	150.0(2)
Pt(3)–Pt(2)–P(2)	148.7(2)	Pt(1)–Pt(3)–P(3)	149.7(2)
Pt(2)–Pt(3)–P(3)	149.2(2)	Pt(2)–Pt(1)–S(1)	51.3(2)
Pt(2)–Pt(1)–S(3)	111.4(2)	Pt(3)–Pt(1)–S(1)	111.4(2)
Pt(3)–Pt(1)–S(3)	51.4(2)	Pt(1)–Pt(2)–S(1)	51.7(3)
Pt(1)–Pt(2)–S(2)	111.6(3)	Pt(3)–Pt(2)–S(1)	111.7(2)
Pt(3)–Pt(2)–S(2)	52.0(3)	Pt(1)–Pt(3)–S(2)	112.0(3)
Pt(1)–Pt(3)–S(3)	52.9(2)	Pt(2)–Pt(3)–S(2)	52.4(3)
Pt(2)–Pt(3)–S(3)	112.8(2)	P(1)–Pt(1)–S(1)	99.5(2)
P(1)–Pt(1)–S(3)	98.0(3)	Pt(2)–Pt(2)–S(1)	99.0(2)
P(2)–Pt(2)–S(2)	98.2(3)	P(3)–Pt(3)–S(2)	98.2(3)
P(3)–Pt(3)–S(3)	97.6(2)	S(1)–Pt(1)–S(3)	162.4(2)
S(1)–Pt(2)–S(2)	162.1(3)	S(2)–Pt(3)–S(3)	162.6(3)
Pt(1)–S(1)–Pt(2)	76.9(2)	Pt(2)–S(2)–Pt(3)	75.6(2)
Pt(1)–S(3)–Pt(3)	75.7(2)	Pt(1)–S(1)–O(1)	114.2(13)
Pt(1)–S(1)–O(2)	116.1(14)	Pt(2)–S(1)–O(1)	112.7(15)
Pt(2)–S(1)–O(2)	113.0(14)	Pt(2)–S(2)–O(3)	120.6(32)
Pt(2)–S(2)–O(4)	114.5(29)	Pt(3)–S(2)–O(3)	122.1(33)
Pt(3)–S(2)–O(4)	108.9(22)	Pt(1)–S(3)–O(5)	114.5(22)
Pt(1)–S(3)–O(6)	109.9(21)	Pt(3)–S(3)–O(5)	115.1(23)
Pt(3)–S(3)–O(6)	110.7(21)	O(1)–S(1)–O(2)	117.2(21)
O(3)–S(2)–O(4)	110.9(39)	O(5)–S(3)–O(6)	121.8(31)

Table 4. Bond distances (Å) and angles (°) for compound (**4d**)

Pt(1)–Pt(1')	2.882 6(8)	Pt(1)–Pt(2)	2.886 8(8)
Pt(1)–P(1)	2.289(3)	Pt(2)–P(2)	2.295(4)
Pt(1)–S(1)	2.247(6)	Pt(1)–S(2)	2.302(6)
Pt(2)–S(2)	2.310(6)	Pt(1)–Br(1)	2.576(4)
Pt(1)–Br(2)	2.495(7)	Pt(2)–Br(2)	2.501(7)
S(1)–O(11)	1.43(2)	S(1)–O(12)	1.42(2)
S(2)–O(21)	1.34(2)	S(2)–O(22)	1.45(2)
Pt(2)–Pt(1)–Pt(1')	60.048(9)	Pt(1)–Pt(2)–Pt(1')	59.90(2)
P(1)–Pt(1)–Pt(1')	149.44(7)	Pt(1)–Pt(1)–Pt(2)	149.62(7)
P(2)–Pt(2)–Pt(1)	149.79(2)	S(1)–Pt(1)–Pt(1')	50.1(1)
S(1)–Pt(1)–Pt(2)	110.1(1)	S(1)–Pt(1)–P(1)	99.8(1)
S(2)–Pt(1)–Pt(1')	111.3(1)	S(2)–Pt(1)–Pt(2)	51.4(1)
S(2)–Pt(1)–P(1)	99.0(2)	S(2)–Pt(1)–S(1)	161.0(2)
S(2)–Pt(2)–Pt(1)	51.1(1)	S(2)–Pt(2)–Pt(1')	110.9(1)
S(2)–Pt(2)–P(2)	99.2(1)	S(2)–Pt(2)–S(2')	160.9(3)
Br(1)–Pt(1)–Pt(1')	55.98(7)	Br(1)–Pt(1)–Pt(2)	114.15(6)
Br(1)–Pt(1)–P(1)	96.17(9)	Br(1)–Pt(1)–S(2)	158.3(2)
Br(2)–Pt(1)–Pt(1')	114.5(1)	Br(2)–Pt(1)–Pt(2)	54.8(2)
Br(2)–Pt(1)–P(1)	94.9(2)	Br(2)–Pt(1)–S(1)	164.1(2)
Br(2)–Pt(2)–Pt(1)	54.6(2)	Br(2)–Pt(2)–Pt(1')	114.2(2)
Br(2)–Pt(2)–P(2)	95.2(2)	Br(2)–Pt(2)–S(2)	165.2(1)
Pt(1)–S(1)–Pt(1')	79.8(3)	O(11)–S(1)–Pt(1)	118.2(8)
O(12)–S(1)–Pt(1)	107.9(7)	O(11)–S(1)–O(12)	118.2(13)
Pt(2)–S(2)–Pt(1)	77.5(2)	O(21)–S(2)–Pt(1)	114.4(8)
O(21)–S(2)–Pt(2)	117.2(8)	O(22)–S(2)–Pt(1)	117.7(8)
O(22)–S(2)–Pt(2)	106.6(8)	O(22)–S(2)–O(21)	119.9(11)
Pt(1)–Br(1)–Pt(1')	68.0(1)	Pt(2)–Br(1)–Pt(1)	70.6(2)

two $\text{Au}(\text{PR}'_3)^+$ groups cap the $\text{Pt}_3(\mu\text{-Cl})(\mu\text{-SO}_2)_2\{\text{P}(\text{C}_6\text{H}_{11})_3\}_3$ triangle, the Pt–Pt distances are 2.864(1) and 2.890(1) Å respectively.

Theoretical calculations^{9,10} have indicated that the transformation from a 42- to 44-electron triangular cluster is associated with the occupation of an orbital of a_2' symmetry, which lies in the plane of the triangle and is weakly metal-metal antibonding. The increase in platinum-platinum bond lengths from $[\text{Pt}_3(\mu\text{-SO}_2)_3\{\text{P}(\text{C}_6\text{H}_{11})_3\}_3]$ to $[\text{Pt}_3(\mu\text{-Br})(\mu\text{-SO}_2)_2\{\text{P}(\text{C}_6\text{H}_{11})_3\}_3]^-$ is consistent with this analysis.

Experimental

Reactions were routinely carried out using standard Schlenk-line procedures under an atmosphere of pure, dry N_2 and using dry dioxygen-free solvents. Microanalyses (Br, Cl, N, C, and H) were carried out by Mr. M. Gascoyne and his staff at this Laboratory. Grating i.r. spectra were recorded as Nujol mulls using a Pye-Unicam SP2000 spectrometer. Fourier-transform i.r. spectra were recorded as Nujol mulls using a Perkin-Elmer 1710 spectrometer.

Proton-decoupled $^{31}\text{P}\{-^1\text{H}\}$ and $^{195}\text{Pt}\{-^1\text{H}\}$ n.m.r. spectra were recorded using a Bruker AM-250 spectrometer. Samples for $^{31}\text{P}\{-^1\text{H}\}$ n.m.r. were referenced to $\text{P}(\text{OMe})_3\text{O}$ in D_2O and for $^{195}\text{Pt}\{-^1\text{H}\}$ n.m.r. to $\text{Na}_2[\text{PtCl}_6]$ in D_2O . The machine operating frequencies were 101.26 MHz for ^{31}P and 53.51 MHz

for ^{195}Pt ; spectra for all samples were run in deuteriated solvents. N.m.r. computer simulations were carried out using the Oxford University VAX computer system using a program developed by Professor R. K. Harris then of the University of East Anglia and adapted for use at Oxford by Dr. A. E. Derome. The compound $[\text{Pt}_3(\mu\text{-CO})_3\{\text{P}(\text{C}_6\text{H}_{11})_3\}_3]\cdot\text{C}_6\text{H}_6$ was synthesised by the method of Clark *et al.*¹⁴ from *trans*- $[\text{PtH}_2\{\text{P}(\text{C}_6\text{H}_{11})_3\}_3]$ and CO .¹⁴

Synthesis of $[\text{Pt}_3(\mu\text{-SO}_2)_3\{\text{P}(\text{C}_6\text{H}_{11})_3\}_3]$ (2).—The complex $[\text{Pt}_3(\mu\text{-CO})_3\{\text{P}(\text{C}_6\text{H}_{11})_3\}_3]\cdot\text{C}_6\text{H}_6$ (0.20 g, 0.13 mmol) was dissolved in benzene (30 cm^3) and the solution warmed to 60 °C. Sulphur dioxide gas was bubbled through this solution for 45 min. Concentration of the solution followed by addition of hexane precipitated orange microcrystals. Yield: 0.14 g (65%) (Found: C, 40.2; H, 6.2. $\text{C}_{60}\text{H}_{105}\text{O}_6\text{P}_3\text{Pt}_3\text{S}_3$ requires C, 40.0; H, 6.1%; $\nu(\text{SO}_2)$ at 1 245mw, 1 081vs, and 1 072s cm^{-1}).

Synthesis of $[\text{Pt}_3(\mu\text{-SO}_2)(\mu\text{-CO})_2\{\text{P}(\text{C}_6\text{H}_{11})_3\}_3]$ (3).—The complex $[\text{Pt}_3(\mu\text{-SO}_2)_3\{\text{P}(\text{C}_6\text{H}_{11})_3\}_3]$ (0.12 g, 0.07 mmol) was dissolved in benzene (20 cm^3) and CO bubbled through the orange solution for 2 min to form a yellow solution. The solvent was removed *in situ* and the solid recrystallised from diethyl

Table 5. Positional parameters ($\times 10^4$) for compound (2)

Atom	X/a	Y/b	Z/c	Atom	X/a	Y/b	Z/c
Pt(1)	2 054.2(5)	1 646.7(4)	1 571.4(4)	G(29)	-2 188(17)	-43(14)	3 406(13)
Pt(2)	963.3(6)	1 025.1(4)	2 393.8(4)	C(30)	-1 306(17)	-272(12)	3 169(13)
Pt(3)	928.4(6)	2 327.3(4)	2 317.6(4)	C(31)	817(14)	-190(10)	3 475(10)
P(1)	3 002(4)	1 628(3)	778(2)	C(32)	1 792(15)	-347(11)	3 403(11)
P(2)	337(4)	124(3)	2 730(3)	C(33)	2 176(20)	-662(14)	4 040(13)
P(3)	270(4)	3 244(3)	2 549(3)	C(34)	2 111(21)	-250(15)	4 589(15)
S(1)	1 944(5)	614(3)	1 754(4)	C(35)	1 220(19)	-54(16)	4 660(14)
S(2)	242(6)	1 708(5)	3 021(4)	C(36)	773(18)	727(12)	4 044(12)
S(3)	1 918(6)	2 712(3)	1 685(4)	C(37)	414(15)	3 867(11)	1 946(11)
O(1)	2 685(18)	351(14)	2 112(17)	C(38)	-129(18)	3 713(12)	1 324(12)
O(2)	1 582(18)	278(14)	1 268(19)	C(39)	58(26)	4 191(16)	794(17)
O(3)	-482(72)	1 690(22)	3 024(33)	C(40)	-71(25)	4 850(18)	1 006(17)
O(4)	747(43)	1 805(47)	3 802(57)	C(41)	427(21)	5 006(16)	1 654(14)
O(5)	2 623(29)	3 009(23)	1 965(27)	C(42)	208(18)	4 509(12)	2 159(13)
O(6)	1 532(29)	2 938(21)	1 146(32)	C(43)	714(14)	3 582(10)	3 275(10)
C(1)	2 928(15)	918(11)	297(11)	C(44)	1 699(17)	3 733(12)	3 261(12)
C(2)	2 074(17)	795(11)	-50(12)	C(45)	2 075(20)	4 034(14)	3 892(13)
C(3)	2 063(18)	130(13)	-332(13)	C(46)	1 906(20)	3 600(14)	4 454(14)
C(4)	2 766(16)	7(14)	-767(12)	C(47)	955(16)	3 475(13)	4 509(12)
C(5)	3 682(17)	142(12)	-436(12)	C(48)	570(16)	3 176(11)	3 888(11)
C(6)	3 686(17)	828(11)	-172(12)	C(49)	-903(15)	3 113(10)	2 676(11)
C(7)	4 158(13)	1 637(11)	1 107(9)	C(50)	-1 366(16)	2 722(11)	2 135(12)
C(8)	4 387(16)	1 051(12)	1 489(12)	C(51)	-2 246(15)	2 551(11)	2 354(12)
C(9)	5 327(19)	1 062(13)	1 753(14)	C(52)	-2 822(16)	3 095(11)	2 534(12)
C(10)	5 517(20)	1 693(15)	2 174(14)	C(53)	-2 307(15)	3 490(11)	3 046(11)
C(11)	5 307(19)	2 214(13)	1 744(14)	C(54)	-1 426(14)	3 692(10)	2 843(11)
C(12)	4 352(18)	2 231(12)	1 496(13)	C(121)	1 167(53)	1 803(39)	4 981(38)
C(13)	2 885(16)	2 334(12)	279(12)	C(122)	1 913(53)	2 103(38)	5 500(38)
C(14)	3 559(19)	2 429(13)	-227(13)	Cl(1)	676(19)	1 608(14)	5 459(13)
C(15)	3 374(22)	3 105(16)	-531(17)	Cl(2)	2 446(26)	1 523(16)	5 487(19)
C(16)	2 408(22)	3 166(21)	-780(19)	C(101)	-165(19)	1 841(24)	534(21)
C(17)	1 787(22)	3 042(15)	-300(16)	C(102)	-660(35)	1 369(15)	881(18)
C(18)	2 014(16)	2 384(13)	-36(14)	C(103)	-1 406(37)	1 370(21)	988(17)
C(19)	448(15)	-514(10)	2 149(10)	C(104)	-1 656(19)	1 843(24)	748(21)
C(20)	-84(16)	-394(11)	1 524(11)	C(105)	-1 161(35)	2 315(15)	401(19)
C(21)	181(21)	-871(13)	1 025(14)	C(106)	-415(37)	2 313(21)	294(17)
C(22)	13(21)	-1 523(15)	1 256(15)	C(111)	3 813(47)	2 034(20)	3 513(26)
C(23)	472(19)	-1 632(16)	1 887(13)	C(112)	4 254(26)	1 663(34)	3 925(30)
C(24)	255(16)	-1 170(10)	2 386(11)	C(113)	3 718(40)	1 165(28)	4 142(21)
C(25)	-786(14)	261(10)	2 893(10)	C(114)	2 741(48)	1 040(20)	3 946(27)
C(26)	-1 353(14)	577(11)	2 338(10)	C(115)	2 300(26)	1 412(34)	3 534(30)
C(27)	-2 200(16)	796(12)	2 573(12)	C(116)	2 836(40)	1 909(28)	3 318(20)
C(28)	-2 716(19)	312(13)	2 861(13)				

ether-methanol gave yellow crystals. Yield: 0.08 g (70%) (Found: C, 46.0; H, 6.5. $C_{62}H_{105}O_4P_3Pt_3S$ requires C, 45.8; H, 6.5%); $\nu(CO)$ at 1 842s and 1 785vs cm^{-1} ; $\nu(SO_2)$ at 1 078w and 1 070s cm^{-1} .

Synthesis of $[NEt_3(CH_2Ph)][Pt_3(\mu-Cl)(\mu-SO_2)_2(PPh_3)_3]$ (4a).—The complex $[Pt_3(\mu-SO_2)_3(PPh_3)_3]$ (0.65 g, 0.04 mmol) was dissolved in benzene-ethanol (4:1, 30 cm^3); $[NEt_3(CH_2Ph)]Cl$ (26 mg, 0.12 mmol) was added with stirring. During the course of the reaction (30 min) the colour of the solution lightened from orange to yellow. The solution was then evaporated under reduced pressure to a small volume (10 cm^3) and hexane added to give a bright yellow precipitate. Recrystallisation from acetone-diethyl ether gave yellow crystals. Yield: 55 mg (84%) (Found: C, 46.6; H, 3.9; Cl, 2.9; N, 0.8. $C_{67}H_{66}ClNO_4Pt_3S_2$ requires C, 46.6; H, 3.9; Cl, 2.1; N, 0.8%); $\nu(SO_2)$ at 1 154s, 1 046 (sh), and 1 027m cm^{-1} .

Synthesis of $[NEt_4][Pt_3(\mu-Br)(\mu-SO_2)_2(PPh_3)_3]$ (4b).—Addition of $[NEt_4]Br$ to $[Pt_3(\mu-SO_2)_3(PPh_3)_3]$ in an analogous manner to that used above gave yellow crystalline solid in 85% yield (Found: C, 43.6; H, 3.80; Br, 4.65. $C_{62}H_{65}BrNO_4P_3Pt_3S_3$ requires C, 44.55; H, 3.80; Br, 4.70%).

Synthesis of $[N(PPh_3)_2][Pt_3(\mu-Cl)(\mu-SO_2)_2\{P(C_6H_{11})_3\}_3]$ (4c).—Addition of $[N(PPh_3)_2]Cl$ in an analogous manner to that used above gave (4c) as a yellow crystalline solid in 85% yield (Found: C, 50.6; H, 6.0; Cl, 1.7; N, 0.7. $C_{90}H_{129}ClNO_4P_5Pt_3S_2$ requires C, 50.8; H, 6.1; Cl, 1.7; N, 0.7%).

Synthesis of $[NEt_4][Pt_3(\mu-Br)(\mu-SO_2)_2\{P(C_6H_{11})_3\}_3]$ (4d).—To a stirred solution of (2) (0.35 g, 0.20 mmol) in benzene (30 cm^3) was added a solution of $[NEt_4]Br$ (0.13 g, 0.62 mmol) in ethanol (10 cm^3) followed by a solution of $Me_3NO \cdot 2H_2O$ (0.07 g, 0.63 mmol) in ethanol (5 cm^3). The solution was stirred for 1 h during which time its colour changed from orange to pale yellow. The solution was then evaporated under reduced

pressure to low volume (10 cm^3) and hexane (40 cm^3) added to give a yellow precipitate. Recrystallisation from CH_2Cl_2 -hexane gave a microcrystalline solid. Yield: 0.33 g (91%) (Found: C, 40.9; H, 6.50; Br, 4.40; N, 0.75. $C_{62}H_{119}BrNO_4P_3Pt_3S_2$ requires C, 40.7; H, 6.50; Br, 4.40; N, 0.75%); $\nu(SO_2)$ at 1 016s and 1 149m cm^{-1} .

Synthesis of $[N(PPh_3)_2][Pt_3(\mu-N_3)(\mu-SO_2)_2\{P(C_6H_{11})_3\}_3]$ (4e).—To a stirred solution of (2) (0.20 g, 0.12 mmol) in benzene (30 cm^3) was added a solution of $[N(PPh_3)_2]N_3$ (0.14 g, 0.24 mmol) in ethanol (10 cm^3). The solution was stirred for 18 h during which time its colour changed from orange to yellow. The solvent was removed *in vacuo* and the residue washed well with water (2 \times 50 cm^3) and diethyl ether (2 \times 30 cm^3). Crude product was extracted into CH_2Cl_2 (15 cm^3), filtered, and hexane (50 cm^3) added to give a yellow crystalline solid. Yield: 0.15 g (75%) (Found: C, 50.8; H, 6.05; N, 2.65. $C_{90}H_{129}N_4O_4P_5Pt_3S_2$ requires C, 50.6; H, 6.05; N, 2.65%); $\nu(SO_2)$ at 1 023s and 1 175m cm^{-1} ; $\nu(N_3)$ at 2 051vs cm^{-1} .

Synthesis of $[N(PPh_3)_2][Pt_3(\mu-Cl)(\mu-SO_2)_2(PMe_2Ph)_3]$ (4f).—Addition of $[N(PPh_3)_2]Cl$ to $[Pt_3(\mu-SO_2)_3(PMe_2Ph)_3]$ in an analogous manner to that used above gave (4f) as a pale yellow crystalline solid in 80% yield (Found: C, 42.6; H, 3.70; Cl, 2.05. $C_{60}H_{63}ClN_5O_4Pt_3S_2$ requires C, 42.3; H, 3.70; Cl, 2.10%); $\nu(SO_2)$ at 1 127s and 1 020m cm^{-1} .

Crystal Structure Determinations of $[Pt_3(\mu-SO_2)_3\{P(C_6H_{11})_3\}_3]$ (2) and $[NEt_4][Pt_3(\mu-Br)(\mu-SO_2)_2\{P(C_6H_{11})_3\}_3]$ (4d).—Crystals of (2) used in the analysis were grown from a benzene-methanol solution of the compound. Isomorphous crystals were obtained when either methylene chloride-methanol or methylene chloride-ethanol mixtures were used, indicating that the crystal packing in this case was not greatly influenced by the solvent included in the lattice. Crystals of (4d) were grown directly from a saturated benzene solution of the salt as nearly colourless (pale yellow tint) bars.

Table 6. Positional parameters ($\times 10^4$) for compound (4d)

Atom	X/a	Y/b	Z/c	Atom	X/a	Y/b	Z/c
Pt(1)	4 153.3(1)	3 027.8(1)	204.0(4)	C(46)	1 663(5)	3 131(8)	1 365(17)
Pt(2)	3 265.8(2)	2 500	495.0(5)	C(51)	2 155(6)	2 500	-993(16)
P(1)	4 549.7(9)	3 749.6(9)	-141(2)	C(52)	2 272(6)	2 958(5)	-1 815(13)
P(2)	2 446(1)	2 500	601(4)	C(53)	2 001(7)	2 947(6)	-3 125(15)
C(11)	4 168(4)	4 202(4)	-1 000(11)	C(54)	2 101(8)	2 500	-3 886(20)
C(12)	3 991(5)	4 038(4)	-2 345(12)	C(61)	3 088(8)	4 764(9)	2 687(32)
C(13)	3 584(6)	4 371(5)	-2 803(15)	C(62)	3 040(10)	5 087(16)	3 641(26)
C(14)	3 755(6)	4 895(5)	-2 856(15)	C(63)	2 833(10)	5 525(13)	3 376(32)
C(15)	3 946(5)	5 065(5)	-1 545(15)	C(64)	2 719(9)	5 626(9)	2 093(37)
C(16)	4 356(5)	4 735(5)	-1 116(15)	C(65)	2 782(10)	5 289(13)	1 242(27)
C(21)	4 725(4)	4 074(4)	1 370(10)	C(66)	2 967(8)	4 850(10)	1 428(24)
C(22)	5 042(5)	3 756(5)	2 261(14)	N(1)	3 965(6)	2 500	4 709(17)
C(23)	5 189(6)	4 014(6)	3 507(13)	C(1)	4 024(9)	2 500	6 150(25)
C(24)	4 766(6)	4 223(6)	4 254(13)	C(2)	3 616(12)	2 500	6 998(33)
C(25)	4 450(5)	4 532(6)	3 383(14)	C(3)	3 970(14)	3 022(14)	4 240(40)
C(26)	4 291(5)	4 260(5)	2 154(13)	C(4)	3 521(9)	3 301(9)	4 689(23)
C(31)	5 133(4)	3 671(4)	-1 011(11)	C(5)	3 591(16)	2 198(15)	1 122(46)
C(32)	5 452(5)	4 131(5)	-1 091(15)	C(7)	4 395(17)	2 699(15)	4 039(48)
C(33)	5 931(4)	3 990(6)	-1 640(14)	C(8)	4 874(11)	2 500	4 494(30)
C(34)	5 898(5)	3 760(7)	-2 975(15)	Br(1)	4 905(2)	2 500	555(6)
C(35)	5 574(6)	3 332(7)	-2 941(15)	Br(2)	3 342(2)	3 407(2)	234(7)
C(36)	5 087(5)	3 453(7)	-2 374(13)	S(1)	4 766(3)	2500	40(10)
C(41)	2 200(4)	3 056(4)	1 387(10)	S(2)	3 399(2)	3 334(2)	576(7)
C(42)	2 370(5)	3 133(5)	2 777(13)	O(11)	5 041(8)	2 500	-1 135(22)
C(43)	2 252(6)	3 635(6)	3 267(16)	O(12)	5 014(7)	2 500	468(53)
C(44)	1 714(8)	3 720(8)	3 225(21)	O(21)	3 346(6)	3 554(6)	864(50)
C(45)	1 550(8)	3 662(9)	1 807(25)	O(22)	3 199(7)	3 556(7)	933(54)

The crystals used in the data collection for both compounds were taken directly from solution and mounted and sealed in 0.5-mm capillary tubes as a precaution against solvent loss.

Unit-cell dimensions were obtained by the least-squares fit of the setting angles of 25 well-centred reflections with $2\theta > 20^\circ$. A monoclinic unit cell was found for (2), the systematic absences $0k0$ ($k = 2n + 1$) and $h0l$ ($h + l = 2n + 1$) uniquely determining the space group as $P2_1/n$ (no. 14, non-standard setting). Compound (4d) was orthorhombic with absences $0kl$ ($k + l = 2n + 1$) and $hk0$ ($h = 2n + 1$) compatible with either the centrosymmetric space groups $Pnma$ (no. 62) or the non-centrosymmetric $Pn2_1a$ (no. 33, non-standard setting).

Data for both (2) and (4d) were collected on an Enraf-Nonius CAD-4 diffractometer using graphite-monochromatised Mo- K_α radiation. Details of data collection and reduction are given in Table 2.

The structure of compound (2) was solved by standard Patterson and Fourier methods and refinement effected by full-matrix least-squares methods. Anisotropic thermal parameters were assigned to all atoms heavier than carbon. Although there were sufficient data to convert the latter, the large additional computation necessary was not deemed worthwhile for the small increase in accuracy that would be afforded to the key structural parameters.

The solvent molecules were rather poorly defined; the dichloromethane molecule was treated with a 50:50 disorder of the carbon and the benzene molecules were refined as rigid groups.

A Chebyshev polynomial weighting scheme with three coefficients was employed resulting in final discrepancy factors of $R = 0.058$ and $R' = 0.072$; other details are given in Table 2. Final atomic co-ordinates are given in Table 5.

The structure of (4d) was initially solved in the more general non-centrosymmetric space group using the above techniques. No single discernible peak for the bridging bromine atom could be seen, three peaks of equal height being located in the bridging positions around the triangle of a pattern and height expected for a statistical disorder of the two sulphurs of the μ -SO₂ ligands and the μ -Br. (Similar disorder of halide and sulphur dioxide bridges has been previously observed.¹⁸)

With a fixed S:Br occupancy of 2:1 at these sites the other non-hydrogen atoms of the structure were located, including two mirror-related benzene molecules and a disordered tetraethylammonium counter ion. The mirror symmetry was not broken by any moiety so refinement was continued in the centrosymmetric space group $Pnma$ which placed both cation and anion on a crystallographic mirror plane. Correlation between the positional parameters for the bromine and sulphur atom pairs was reduced by refining the sums and differences of the S and Br co-ordinates rather than the co-ordinates themselves. Bond length restraints of Pt-S 2.29(3) and Pt-Br 2.48(3) Å were used to aid convergence to a chemically reasonable geometry as based on previous structural data. Using this model, the oxygen atoms were located easily.

The structure was then refined (block matrix) with all atoms anisotropic with the exception of the disordered $[\text{NEt}_4]^+$ cation, the Br and SO₂ bridges and the hydrogen atoms, the co-ordinates of which were calculated ($d_{\text{C-H}} = 1.0$ Å, $U_{\text{iso}} = 0.1$ Å³). For 4 291 reflections and using 388 least-squares parameters, the structure converged to $R = 0.044$, $R' = 0.050$. Final atomic co-ordinates are given in Table 6.¹⁹

All calculations for both structure determinations were carried out on a VAX 11-750 computer using the CRYSTALS X-ray program package.

Additional material available from the Cambridge Crystallographic Data Centre comprises thermal parameters, remaining bond parameters.

Acknowledgements

We thank the S.E.R.C. for financial support and Johnson-Matthey plc for a generous loan of platinum metal salts.

References

- 1 T-Y. Luh, *Coord. Chem. Rev.*, 1984, **60**, 225.
- 2 U. Koelle, *J. Organomet. Chem.*, 1977, **133**, 53.
- 3 J. R. Malpass, in 'Comprehensive Organic Chemistry,' ed. E. O. Sutherland, Pergamon Press, Oxford, 1979, vol. 2, p. 40.
- 4 M. F. Hallam and D. M. P. Mingos, *J. Organomet. Chem.*, 1968, **315**, C35.
- 5 D. M. P. Mingos and R. W. M. Wardle, *Transition Met. Chem.*, 1985, **10**, 441.
- 6 J. Chatt and P. Chini, *J. Chem. Soc. A*, 1970, 1538.
- 7 C. E. Briant, D. G. Evans, and D. M. P. Mingos, *J. Chem. Soc., Dalton Trans.*, 1986, 1535.
- 8 C. E. Briant, D. I. Gilmour, D. M. P. Mingos, and R. W. M. Wardle, *J. Chem. Soc., Dalton Trans.*, 1985, 1693.
- 9 D. J. Underwood, R. Hoffman, K. Tatsumi, A. Nakamura, and Y. Yamamoto, *J. Am. Chem. Soc.*, 1985, **107**, 5968.
- 10 D. I. Gilmour and D. M. P. Mingos, *J. Organomet. Chem.*, 1986, **302**, 127.
- 11 J. C. Calabrese, L. F. Dahl, P. Chini, G. Longoni, and J. Martinengo, *J. Am. Chem. Soc.*, 1974, **96**, 2614.
- 12 A. Moor, P. J. Pregosin, and L. M. Venanzi, *Inorg. Chim. Acta*, 1981, **48**, 153; 1982, **61**, 135.
- 13 M. F. Hallam, N. D. Howells, D. M. P. Mingos, and R. W. M. Wardle, *J. Chem. Soc., Dalton Trans.*, 1985, 845.
- 14 H. C. Clark, A. B. Goel, and C. S. Wong, *Inorg. Chim. Acta*, 1979, **34**, 159.
- 15 D. M. Duggan and D. N. Hendrickson, *Inorg. Chem.*, 1973, **12**, 2422.
- 16 D. C. Moody and R. R. Ryan, *Inorg. Chem.*, 1977, **16**, 1052.
- 17 A. Albinati, *Inorg. Chim. Acta*, 1977, **22**, L31.
- 18 O. J. Ezomo, D. M. P. Mingos, and I. D. Williams, unpublished work.
- 19 D. J. Watkin, J. R. Carruthers, and P. W. Betteridge, CRYSTALS User Guide, Chemical Crystallography Laboratory, University of Oxford, 1985.

Received 16th July 1987; Paper 7/1271